Supporting information for: Importance of the Kinetic Energy Density for Band Gap Calculations in Solids with Density Functional Theory

Fabien Tran* and Peter Blaha

Institute of Materials Chemistry, Vienna University of Technology, Getreidemarkt 9/165-TC, A-1060 Vienna, Austria

E-mail: tran@theochem.tuwien.ac.at

*To whom correspondence should be addressed

Table S1: Experimental[S1–S4] lattice constants (in Å) and angles (in degrees) of the unit cell for the solids considered in this work. When necessary, the positions of atoms (in internal units) are indicated at the second line. The space group number is indicated in parenthesis. For Cr_2O_3, Fe_2O_3, MnO, FeO, CoO and NiO, the antiferromagnetic order leads to a lowering of the symmetry (second indicated space group).

solid	a	b	c	α	β	γ
Ne (225)	4.470	4.470	4.470	90	90	90
Ar (225)	5.260	5.260	5.260	90	90	90
Kr (225)	5.640	5.640	5.640	90	90	90
Xe (225)	6.130	6.130	6.130	90	90	90
C (227)	3.567	3.567	3.567	90	90	90
Si (227)	5.430	5.430	5.430	90	90	90
Ge (227)	5.652	5.652	5.652	90	90	90
Al_2O_3 (167)	4.757	4.757	12.988	90	90	120
Al(0,0,0.35218), O(0.30625,0,1/4)						
SiC (216)	4.358	4.358	4.358	90	90	90
SiO_2 (α-quartz,152)	4.921	4.921	5.400	90	90	120
Si(0.528,0,1/3), O(0.408,0.143,0.1193)						
SiO_2 (β-cristobalite,227)	7.126	7.126	7.126	90	90	90
BN (216)	3.616	3.616	3.616	90	90	90
BP (216)	4.538	4.538	4.538	90	90	90
BAs (216)	4.777	4.777	4.777	90	90	90
AlN (216)	4.342	4.342	4.342	90	90	90
AlN (wurtzite,186)	3.111	3.111	4.978	90	90	120
Al(1/3,2/3,0), N(1/3,2/3,0.385)						
AlP (216)	5.463	5.463	5.463	90	90	90
AlAs (216)	5.661	5.661	5.661	90	90	90
AlSb (216)	6.136	6.136	6.136	90	90	90
GaN (216)	4.523	4.523	4.523	90	90	90
GaN (wurtzite,186)	3.180	3.180	5.166	90	90	120
Ga(1/3,2/3,0), N(1/3,2/3,0.385)						
GaP (216)	5.451	5.451	5.451	90	90	90
GaSb (216)	6.096	6.096	6.096	90	90	90
GaAs (216)	5.648	5.648	5.648	90	90	90
InN (wurtzite,186)	3.533	3.533	5.693	90	90	120
In(1/3,2/3,0), N(1/3,2/3,0.385)						
InP (216)	5.869	5.869	5.869	90	90	90
InAs (216)	6.058	6.058	6.058	90	90	90
InSb (216)	6.479	6.479	6.479	90	90	90
SnO_2 (136)	4.737	4.737	3.186	90	90	90
Sn(0,0,0), O(0.30562,0.30562,0)						
SnSe (62)	11.500	4.154	4.446	90	90	90
Sn(0.618,1/4,0.3957), Se(0.3559,1/4,0.0164)						
SnTe (225)	6.318	6.318	6.318	90	90	90
Sb_2Te_3 (166)	4.264	4.264	30.458	90	90	120
Sb(0,0,0.3988), Te1(0,0,0.7872), Te2(0,0,0)						
LiH (225)	4.084	4.084	4.084	90	90	90
LiF (225)	4.010	4.010	4.010	90	90	90
LiCl (225)	5.106	5.106	5.106	90	90	90
NaF (225)	4.609	4.609	4.609	90	90	90
NaCl (225)	5.595	5.595	5.595	90	90	90
KF (225)	5.347	5.347	5.347	90	90	90
KCl (225)	6.293	6.293	6.293	90	90	90
BeO (wurtzite,186)	2.694	2.694	4.384	90	90	120
Be(1/3,2/3,0), O(1/3,2/3,0.3778)						
MgO (225)	4.207	4.207	4.207	90	90	90
MgS (216)	5.622	5.622	5.622	90	90	90
MgSe (225)	5.400	5.400	5.400	90	90	90
MgTe (216)	6.420	6.420	6.420	90	90	90
CaO (225)	4.811	4.811	4.811	90	90	90
CaF_2 (225)	5.463	5.463	5.463	90	90	90
BaS (225)	6.389	6.389	6.389	90	90	90
BaSe (225)	6.595	6.595	6.595	90	90	90
BaTe (225)	7.007	7.007	7.007	90	90	90
ScN (225)	4.500	4.500	4.500	90	90	90
TiO_2 (rutile,136)	4.594	4.594	2.959	90	90	90
Ti(0,0,0), O(0.305,0.305,0)						
TiO_2 (anatase,141)	3.785	3.785	9.512	90	90	90
Ti(0,1/4,3/8), O(1/2,3/4,0.08314)						
$SrTiO_3$ (221)	3.901	3.901	3.901	90	90	90
VO_2 (M_1,14)	5.743	4.517	5.375	90	122.6	90
V(0.242,0.975,0.025), O1(0.1,0.21,0.2), O2(0.39,0.69,0.29)						
Cr_2O_3 (167,146)	4.953	4.953	13.588	90	90	120
Cr(0,0,0.3475), O(0.3058,0,1/4)						
Fe_2O_3 (167,146)	5.035	5.035	13.747	90	90	120
Fe(0,0,0.35534), O(0.3056,0,1/4)						
MnO (225,166)	4.445	4.445	4.445	90	90	90
FeO (225,166)	4.334	4.334	4.334	90	90	90
CoO (225,166)	4.254	4.254	4.254	90	90	90
NiO (225,166)	4.171	4.171	4.171	90	90	90

Table S1: continued

solid	a	b	c	α	β	γ
Cu_2O (224)	4.267	4.267	4.267	90	90	90
CuSCN (160)	3.856	3.856	16.452	90	90	120
Cu(0,0,0), S(0.28904,0.28904,0.28904), C(0.18674,0.18674,0.18674), N(0.1169,0.1169,0.1169)						
CuCl (216)	5.501	5.501	5.501	90	90	90
CuBr (216)	5.820	5.820	5.820	90	90	90
CuI (216)	6.063	6.063	6.063	90	90	90
ZnO (wurtzite,186)	3.258	3.258	5.220	90	90	120
Zn(1/3,2/3,0), O(1/3,2/3,0.382)						
ZnS (216)	5.409	5.409	5.409	90	90	90
ZnSe (216)	5.668	5.668	5.668	90	90	90
ZnTe (216)	6.089	6.089	6.089	90	90	90
MoS_2 (194)	3.160	3.160	12.294	90	90	120
Mo(1/3,2/3,1/4), S(1/3,2/3,0.621)						
AgCl (225)	5.546	5.546	5.546	90	90	90
AgBr (225)	5.772	5.772	5.772	90	90	90
AgI (216)	6.499	6.499	6.499	90	90	90
CdS (216)	5.818	5.818	5.818	90	90	90
CdSe (216)	6.052	6.052	6.052	90	90	90
CdTe (216)	6.480	6.480	6.480	90	90	90

References

(S1) ICSD, Inorganic Crystal Structure Database, http://icsd.fiz-karlsruhe.de (accessed January, 2017).

(S2) American Mineralogist Crystal Structure Database, http://rruff.geo.arizona.edu/AMS/amcsd.php (accessed January, 2017).

(S3) Heyd, J.; Peralta, J. E.; Scuseria, G. E.; Martin, R. L. Energy Band Gaps and Lattice Parameters Evaluated with the Heyd-Scuseria-Ernzerhof Screened Hybrid Functional. *J. Chem. Phys.* **2005**, *123*, 174101.

(S4) Crowley, J. M.; Tahir-Kheli, J.; Goddard, W. A., III Resolution of the Band Gap Prediction Problem for Materials Design. *J. Phys. Chem. Lett.* **2016**, *7*, 1198–1203.

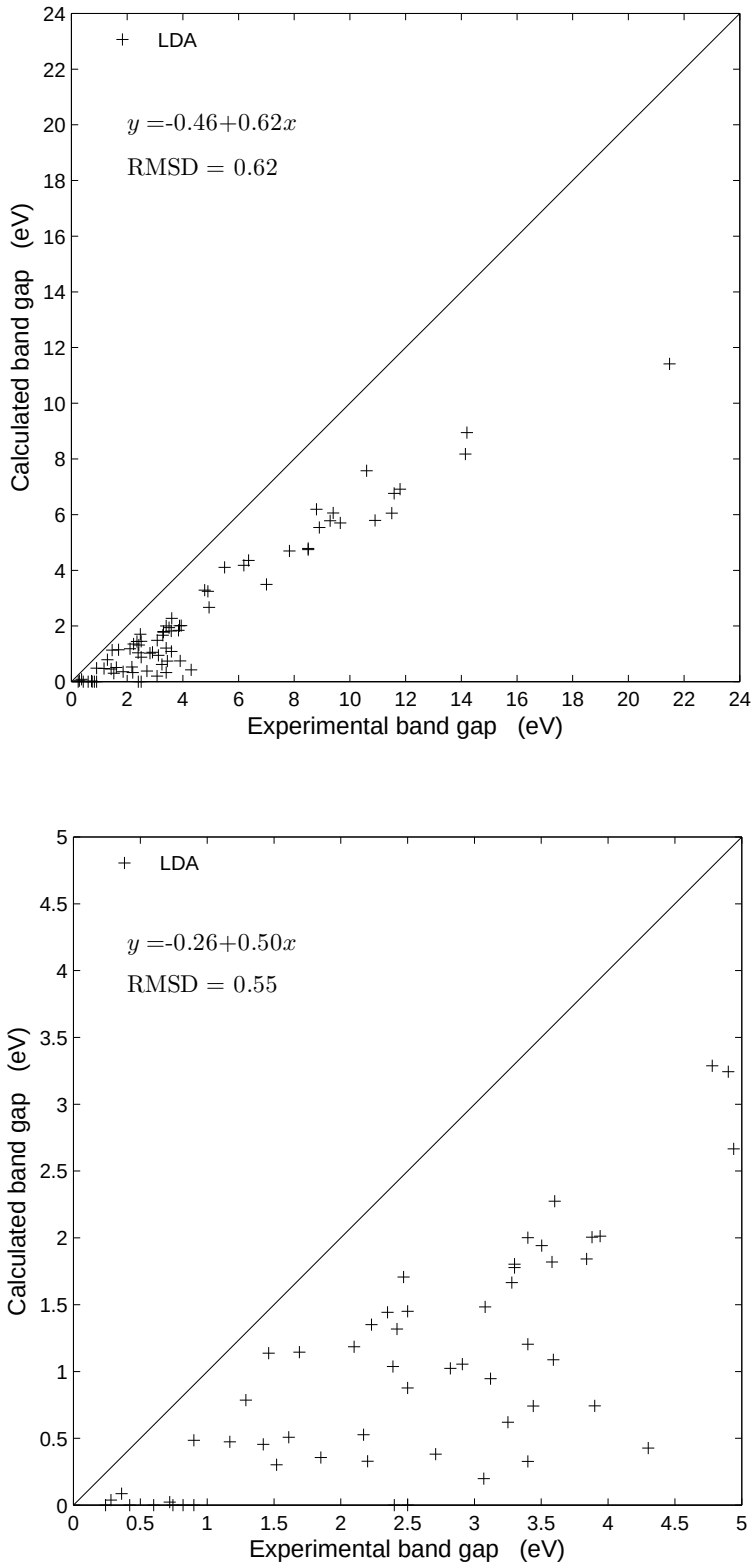

Figure S1: Calculated versus experimental band gaps for the set of 76 solids. The lower panel is a zoom of the upper panel focusing on band gaps smaller than 5 eV. The linear regression and root-mean-square deviation of the data are also shown.

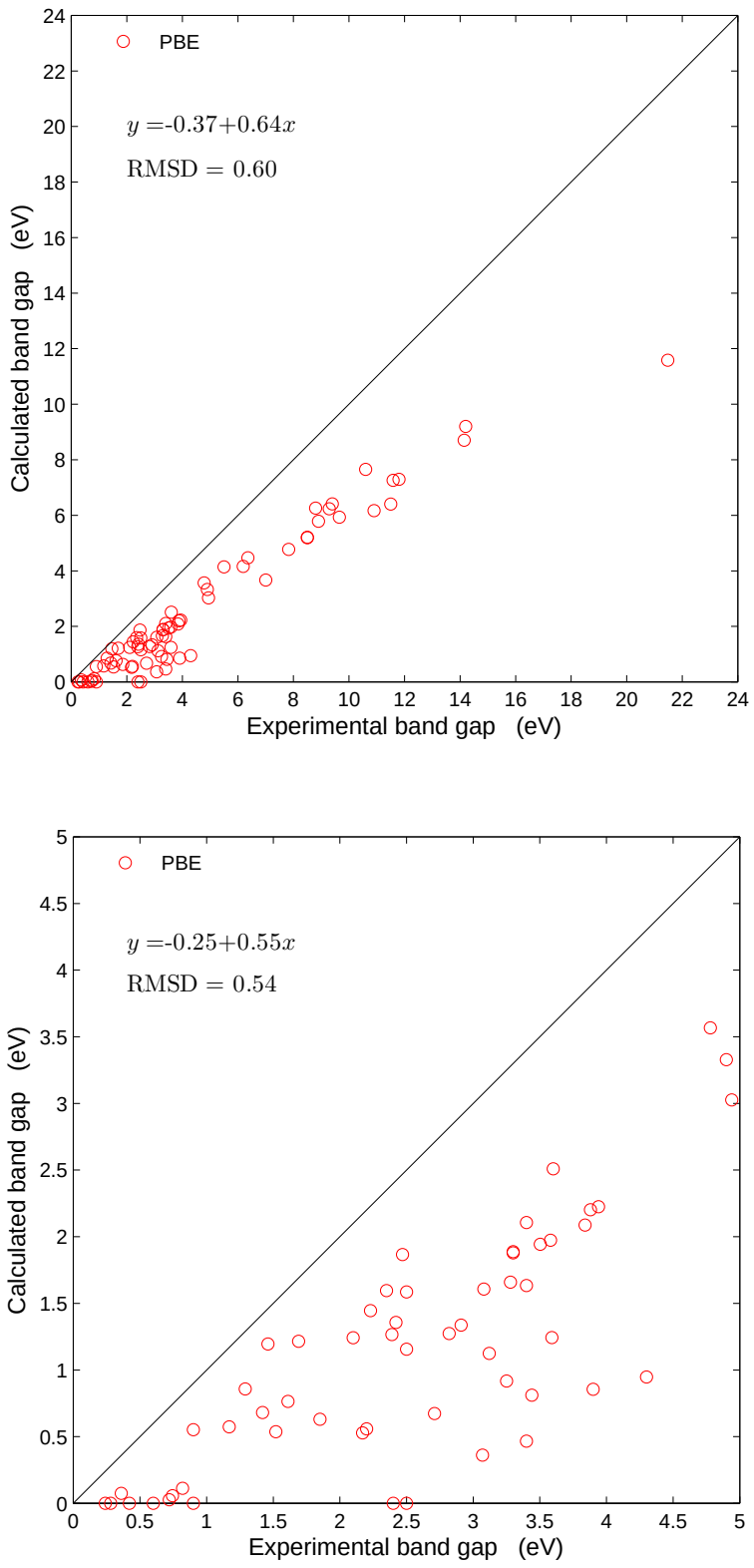

Figure S2: Calculated versus experimental band gaps for the set of 76 solids. The lower panel is a zoom of the upper panel focusing on band gaps smaller than 5 eV. The linear regression and root-mean-square deviation of the data are also shown.

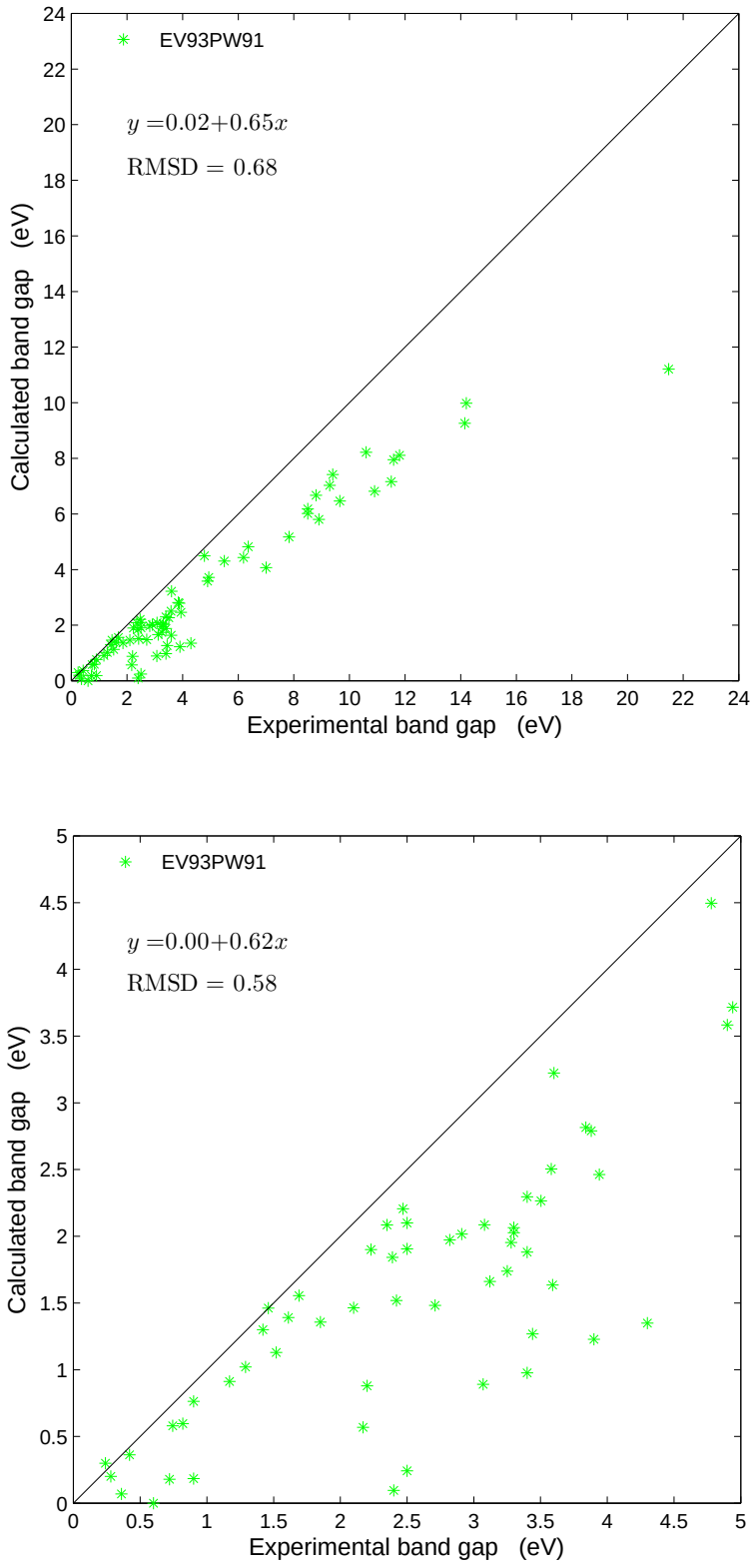

Figure S3: Calculated versus experimental band gaps for the set of 76 solids. The lower panel is a zoom of the upper panel focusing on band gaps smaller than 5 eV. The linear regression and root-mean-square deviation of the data are also shown.

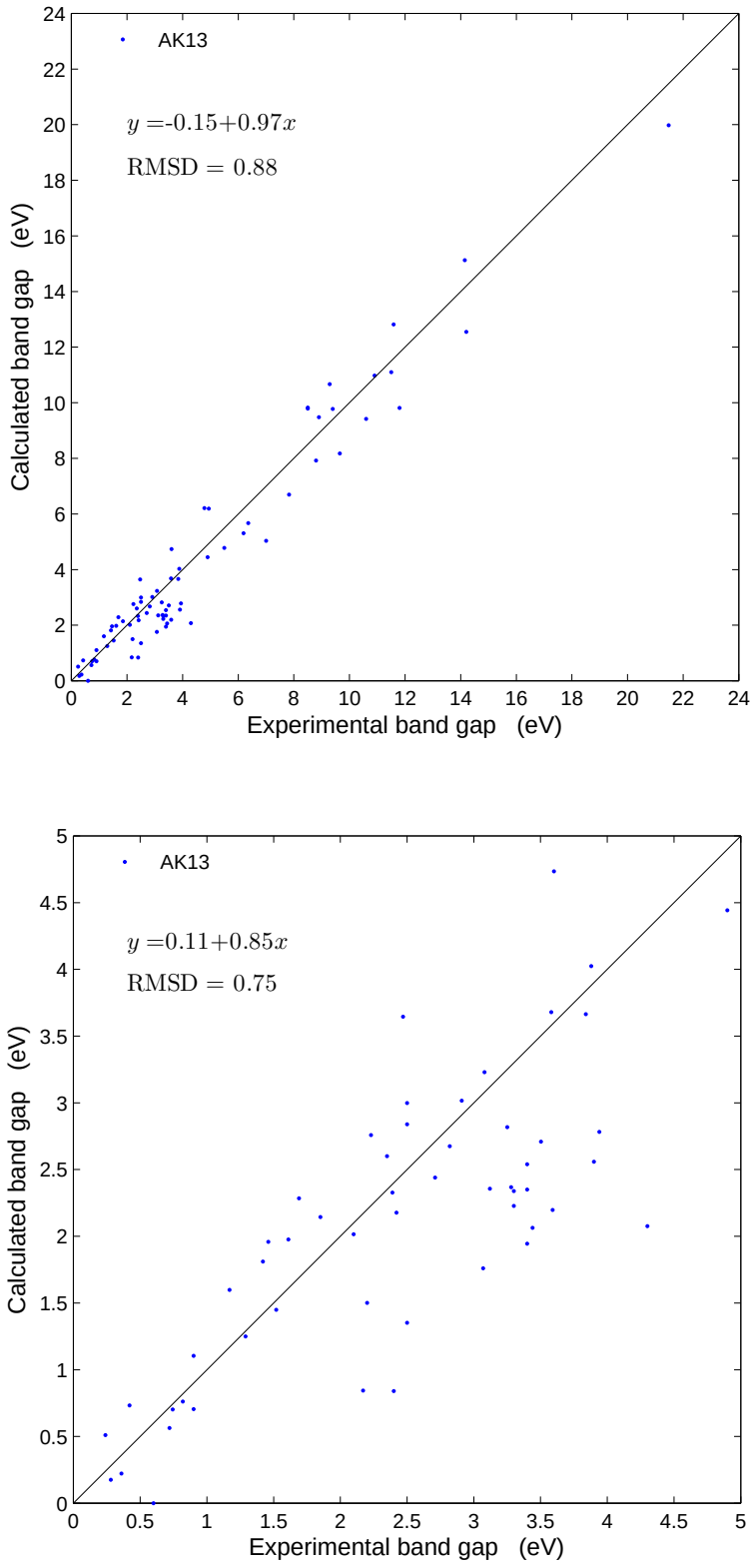

Figure S4: Calculated versus experimental band gaps for the set of 76 solids. The lower panel is a zoom of the upper panel focusing on band gaps smaller than 5 eV. The linear regression and root-mean-square deviation of the data are also shown.

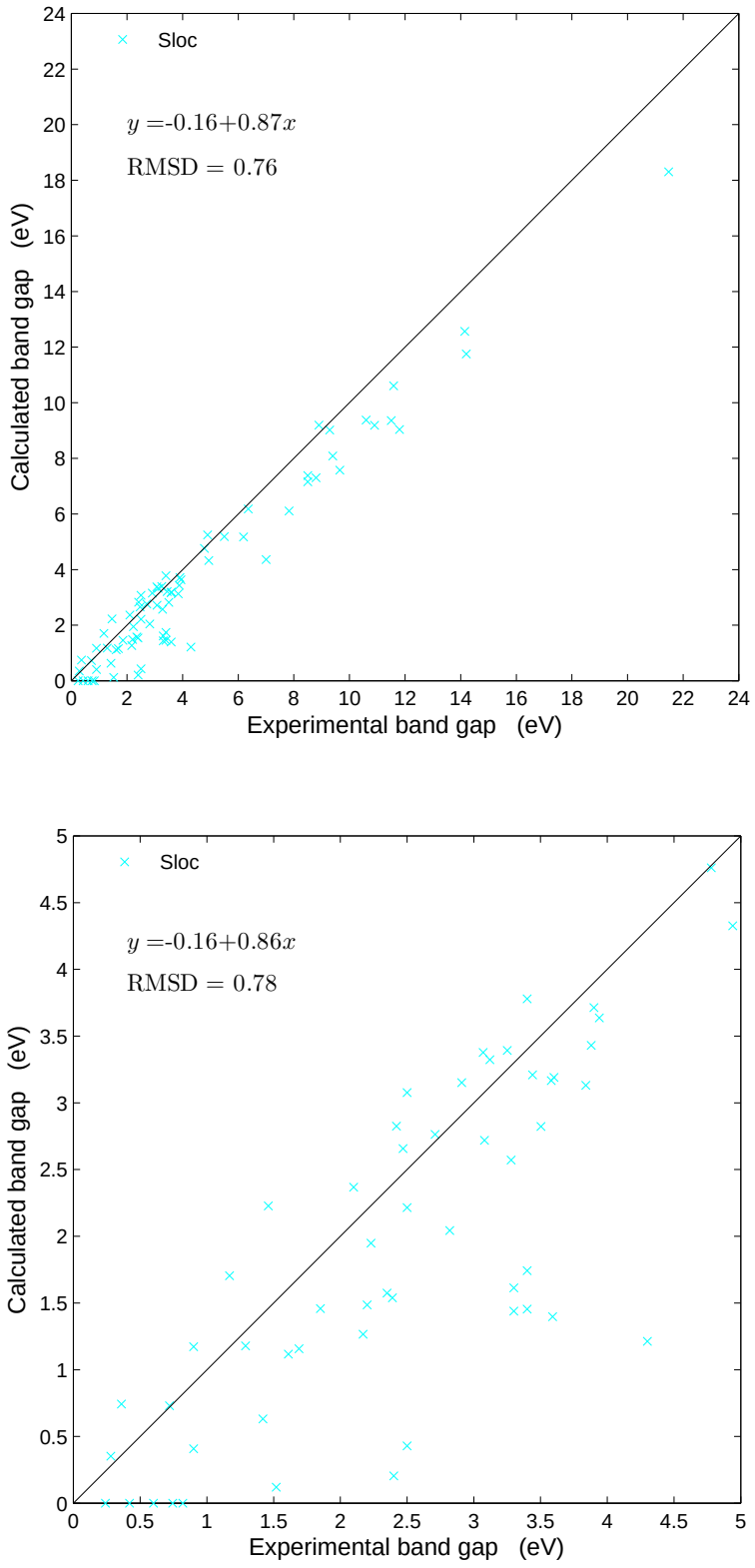

Figure S5: Calculated versus experimental band gaps for the set of 76 solids. The lower panel is a zoom of the upper panel focusing on band gaps smaller than 5 eV. The linear regression and root-mean-square deviation of the data are also shown.

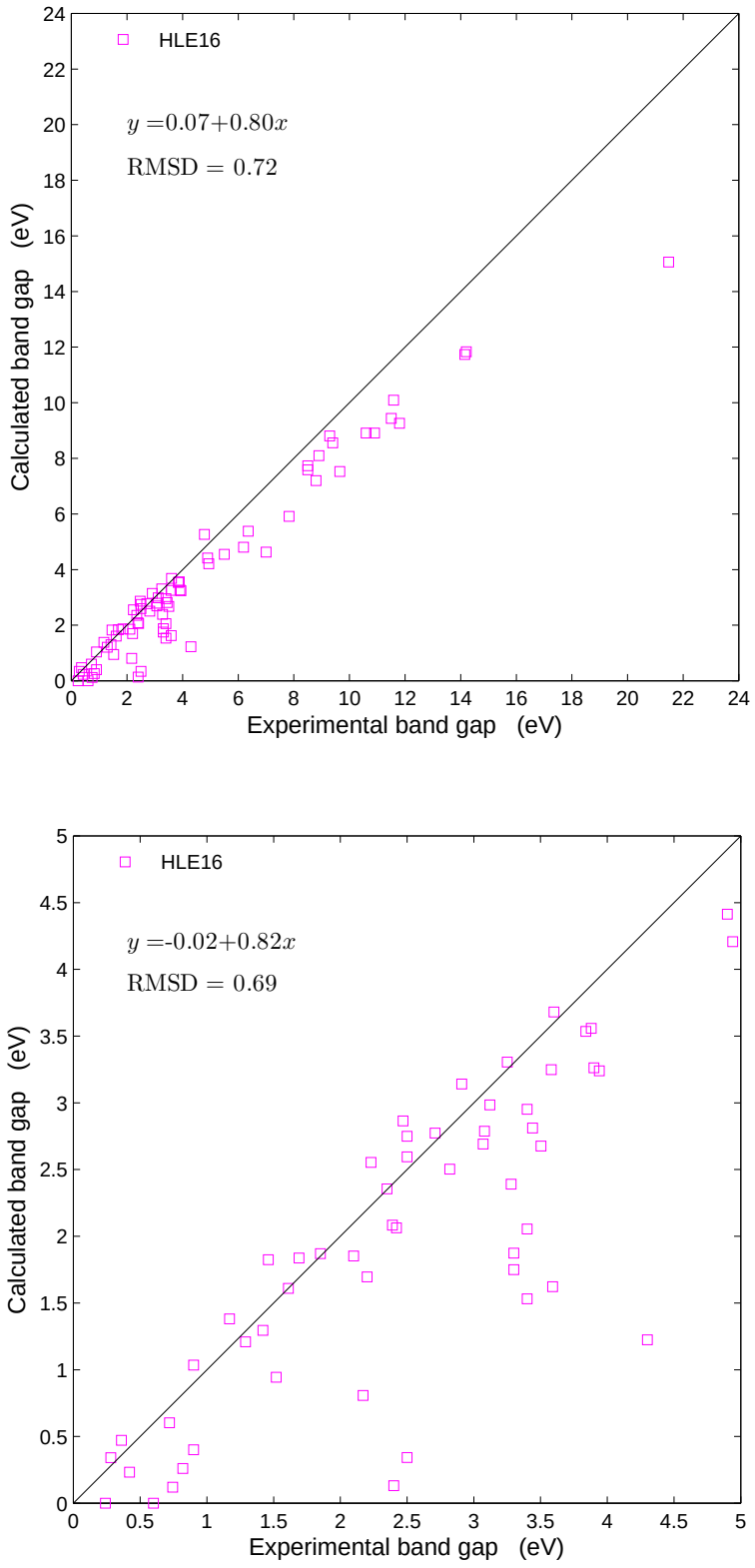

Figure S6: Calculated versus experimental band gaps for the set of 76 solids. The lower panel is a zoom of the upper panel focusing on band gaps smaller than 5 eV. The linear regression and root-mean-square deviation of the data are also shown.

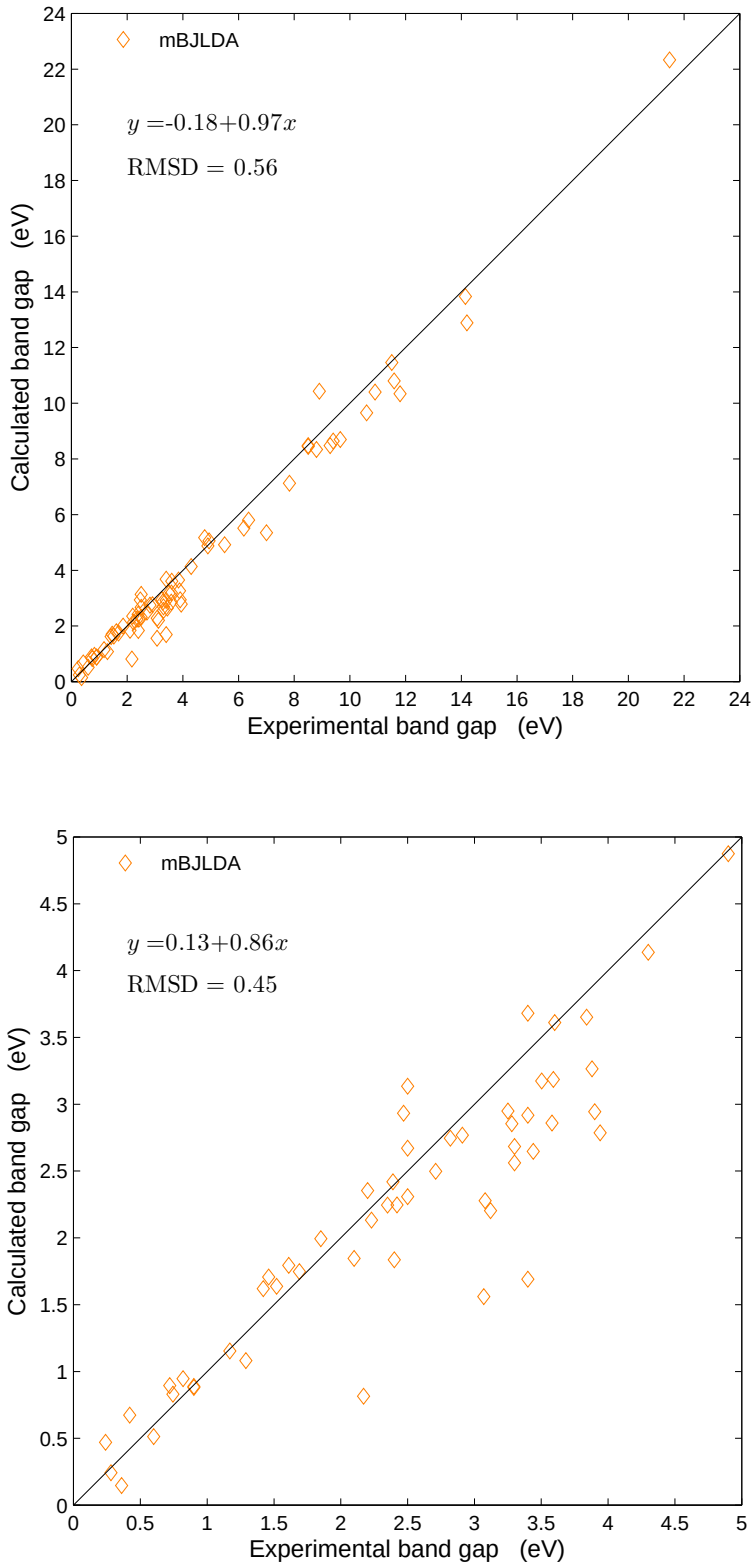

Figure S7: Calculated versus experimental band gaps for the set of 76 solids. The lower panel is a zoom of the upper panel focusing on band gaps smaller than 5 eV. The linear regression and root-mean-square deviation of the data are also shown.

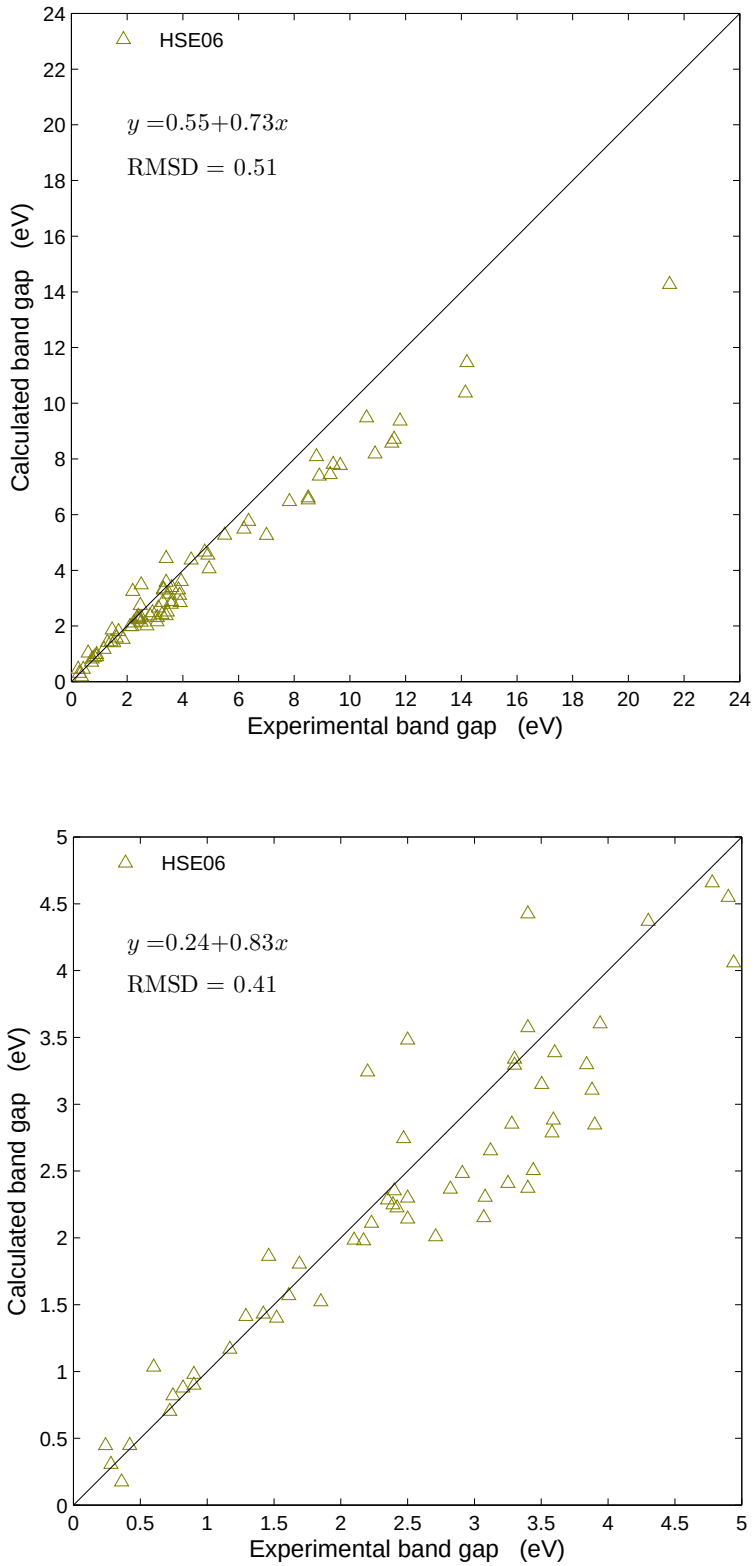

Figure S8: Calculated versus experimental band gaps for the set of 76 solids. The lower panel is a zoom of the upper panel focusing on band gaps smaller than 5 eV. The linear regression and root-mean-square deviation of the data are also shown.

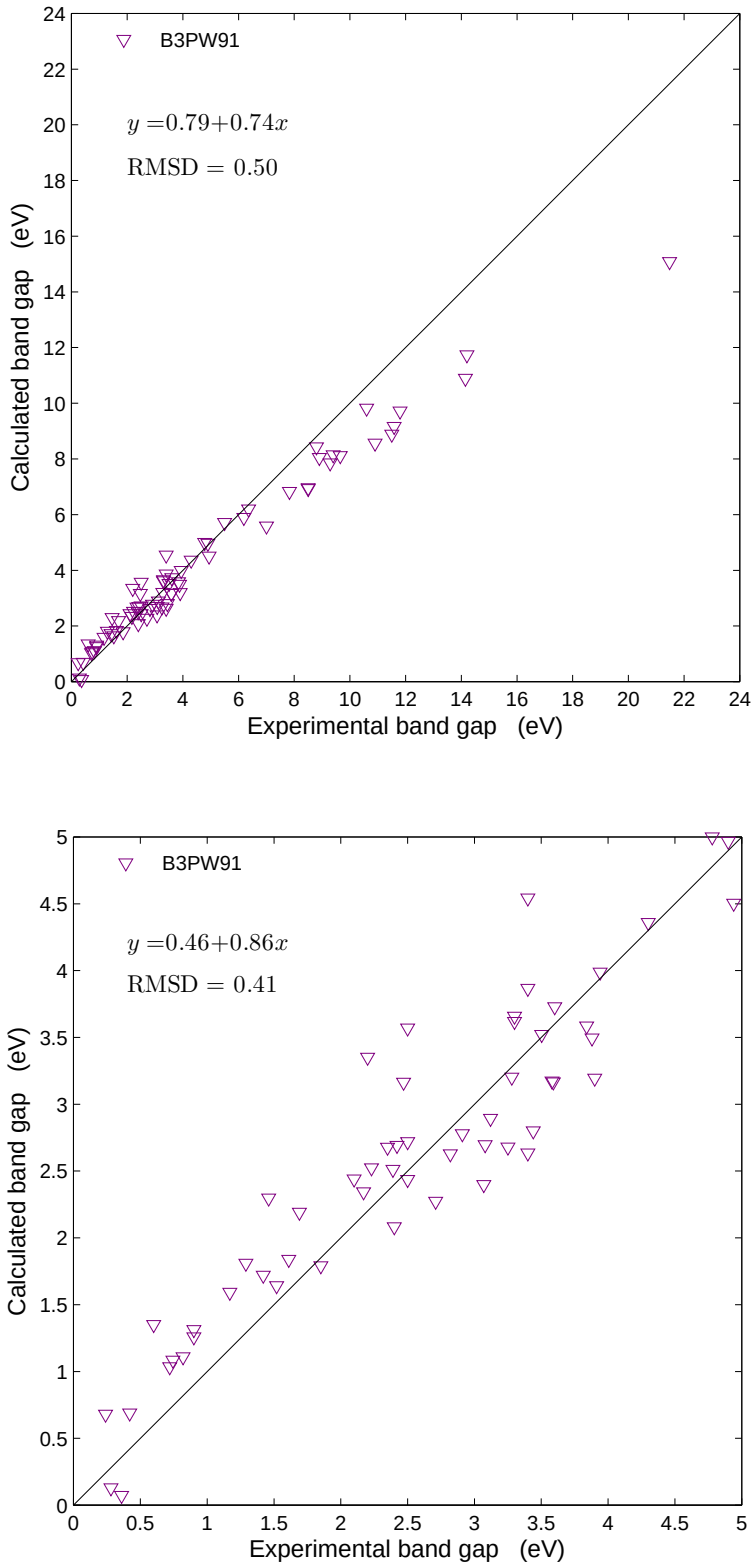

Figure S9: Calculated versus experimental band gaps for the set of 76 solids. The lower panel is a zoom of the upper panel focusing on band gaps smaller than 5 eV. The linear regression and root-mean-square deviation of the data are also shown.